

## Isotropic collision-induced scattering from high-temperature gaseous mercury

M. Sampoli,<sup>1,2</sup> F. Hensel,<sup>3</sup> and F. Barocchi<sup>1,4</sup>

<sup>1</sup>*Istituto Nazionale per la Fisica della Materia (INFN), I-16152 Genova, Italy*

<sup>2</sup>*Dipartimento di Energetica, Università di Firenze, Via Santa Marta 3, Firenze I-50139, Italy*

<sup>3</sup>*Institute of Physical Chemistry and Material Science Center, Philipps University of Marburg, Hans-Meerwein-Strasse, Marburg, Germany*

<sup>4</sup>*Dipartimento di Fisica, Università di Firenze, Largo Enrico Fermi 2, Firenze I-50125, Italy*

(Received 27 September 1995)

We have measured the isotropic collision-induced light-scattering spectrum of a metal vapor, i.e., mercury vapor at temperature  $T=973$  K and densities around  $0.113$  atom/nm<sup>3</sup>, by means of an apparatus which allows us to perform comparisons between polarized and depolarized Raman spectra in high-temperature high-pressure gases and metal vapors. We have then derived an empirical model for the collision-induced polarizability trace of mercury diatom. Similarly to the anisotropy, the obtained trace behaves rather differently from the noble-gas counterpart, showing strong contributions from the electron correlations in the overlap region. [S1050-2947(96)03005-3]

PACS number(s): 34.30+h, 33.20.Fb, 34.20.-b

Collision-induced light-scattering (CILS) spectroscopy has been demonstrated to be a very useful tool to investigate the form of pair Interaction-Induced (I-I) polarizabilities and interaction potentials [1,2]. Most investigations have been devoted to studying the anisotropic part of the I-I polarizability tensor which is directly related to the CILS depolarized spectrum. The study of the I-I isotropic polarizability, i.e., of the trace of the I-I polarizability tensor, is a much more difficult task, both experimentally and theoretically. Indeed, experimentally the I-I polarizability trace contributes to the CILS polarized spectrum only marginally, the corresponding anisotropic part being usually responsible for most of the spectral integrated intensity. The first experimental determination of the spectrum due to the I-I isotropic polarizability was performed in noble gases by Proffitt, Keto, and Frommhold [3] and in a molecular system by De Santis and Sampoli [4].

Experimentally, the signal due to the polarizability trace, which from now on we call the "isotropic spectrum" [6], is derived from a small difference of two already weak signals, which have to be calibrated relative to each other with high precision. This brought large uncertainties from 25% to more than 100% on the spectral intensity of noble gases.

Theoretically, the difficulties in the calculation come mainly from large cancellations between the various contributions to the trace. In turn, this fact makes the calculations of the trace both a theoretical challenge and a stringent test of the employed wave functions, respectively. The empirical and theoretical models for the I-I polarizability trace of noble gases from helium to xenon have been extensively discussed by Dacre and Frommhold [5].

The difficulties in detecting the isotropic spectrum for systems composed by particles with spherical symmetry can readily be understood by recalling that, in first approximation, i.e., by considering only the lowest-order dipole-induced-dipole (DID) terms for the I-I polarizabilities, the ratio of the isotropic to anisotropic integrated intensity is of the order of  $10(\alpha/r_m^3)^2/3$ , where  $\alpha$  is the particle polarizability and  $r_m$  the pair distance at the potential minimum [7]. For

He, Ne, Ar, Kr, and Xe this ratio yields  $2.5 \times 10^{-4}$ ,  $6 \times 10^{-4}$ ,  $3 \times 10^{-3}$ ,  $5 \times 10^{-3}$ , and  $8 \times 10^{-3}$ , respectively.

Recently, CILS depolarized spectra of mercury vapor have been measured at various temperatures [8–11] and an empirical model for the I-I polarizability anisotropy has been extracted [12]. In mercury, differently from noble gases, we found, beside the usual DID term, an additional long-range contribution to the polarizability anisotropy which has been attributed to the onset of electron correlation in the outer shells. This peculiarity together with the large  $\alpha$  and small  $r_m$  (due to the relativistic behavior of mercury electrons) makes mercury a very interesting case for studying the isotropic spectrum. For mercury,  $\alpha_{\text{Hg}}=5.7 \text{ \AA}^3$ ,  $r_{\text{Hg},m}=3.6 \text{ \AA}$ , and the ratio  $10(\alpha_{\text{Hg}}/r_{\text{Hg},m}^3)^2/3$  gives  $5 \times 10^{-2}$ , therefore this atomic system is one of the best cases for measuring the isotropic spectrum. However, there are severe experimental difficulties in performing Raman scattering from high-purity metal vapor at high temperature and pressure.

Here we report measurements of the collision-induced isotropic light-scattering spectrum of a metal diatom, i.e., mercury, in the range  $6\text{--}70 \text{ cm}^{-1}$ , and we present an empirical model for the I-I polarizability trace of mercury. This high-temperature spectroscopy can be applied to several metal vapors and is the only available experimental method for studying the I-I trace of a metal diatom. The experiment has been performed with an apparatus designed for high-temperature ( $\approx 900 \text{ }^\circ\text{C}$ ) and high-pressure (100 MPa) Raman spectroscopy of gases, which has already been described in some detail in recent works [8,11]. Here, the only differences worth mentioning are (i) the use of an image rotator in order to rotate the polarization of the incoming beam in the two required geometries, i.e., either normal to the scattering plane or along the collecting optical axis; and (ii) the addition inside the sample cell of a small amount of nitrogen for calibrating both CILS spectra against the rotational spectrum of nitrogen. We want to recall two relevant characteristics of our apparatus: (i) the windows of the scattering cell are made of fused quartz and do not depolarize the incoming laser beam and the scattered light even at the highest working

temperatures, as has carefully been checked; and (ii) the scattered light is collected in a small cone of about  $\pm 3^\circ$ . These two characteristics ensure that the leakage of unwanted polarizations is negligible in our case, less than 1%, different from previous experiments in noble gases.

The spectra were measured with a power of 1 W at 488 nm from an argon ion laser. The scattering angle was  $90^\circ$  and the scattering plane was horizontal. The laser beam was polarized either in the vertical or horizontal direction and focused into the sample cell. The scattered light was selected always with vertical polarization by means of a Polaroid sheet. The isotropic spectrum  $I_{\text{iso}}(\nu)$  is derived from the measured spectra by

$$I_{\text{iso}}(\nu) = I_{VV}(\nu) - \frac{4}{3} I_{HV}(\nu), \quad (1)$$

where  $I_{VV}(\nu)$  and  $I_{HV}(\nu)$  are the scattered intensities when the laser beam is polarized vertically and horizontally, respectively. The  $VV$  and  $HV$  intensities of the mercury have been measured separately at  $T = 973 \pm 2$  K and three different densities, namely, 0.065, 0.113, and 0.141 atom/nm<sup>3</sup>; the intensities are found to be quadratic in density within experimental uncertainties, indicating that all the spectra are to be attributed to I-I diatomic polarizability. The overall response of the apparatus has been calibrated against a blackbody radiation source and during the experiment the power of the laser beam transmitted through the sample cell has been monitored.

The main difficulty for precise measurements of the isotropic signal is caused by the change in the optical alignment when the incoming polarization is rotated from vertical to horizontal direction. These changes may alter spuriously the weak isotropic contribution. In order to control these modifications as much as possible we have chosen to calibrate both spectra with an internal standard. To this purpose we have mixed a small quantity of nitrogen with the mercury vapor and recorded in the same run the induced spectra of mercury and the rotational spectrum of nitrogen. The rotational spectrum of nitrogen is known to be completely depolarized at low density in the 1–300 cm<sup>-1</sup> region. We can estimate that the small quantity of nitrogen we have used does not contribute appreciably to the measured isotropic intensity. Indeed, in the DID two-body approximation, the ratio between the largest isotropic contribution due to nitrogen-mercury collisions with respect to mercury-mercury ones is proportional to  $(\alpha_{N_2}/\alpha_{Hg})^2 \rho_{N_2}/\rho_{Hg}$  where the isotropic polarizability of the nitrogen molecule is  $\alpha_{N_2} = 1.76 \text{ \AA}^3$  [13], while  $\rho$  stands for the particle density. In our case this ratio has always been less than 3%, rather smaller than the experimental uncertainties of our measurements. With the addition of nitrogen we have been able to calibrate the  $VV$  and  $HV$  spectra from the knowledge of the absolute intensity of the rotational lines (the polarizability anisotropy of nitrogen [13] being  $\beta_{N_2} = 0.69 \text{ \AA}^3$ ) and to ascertain that no alignment change was detectable with our apparatus, since the ratio of the integrated intensity of each rotational line between the two polarizations was equal to the theoretical value  $\frac{3}{4}$  within 1%.

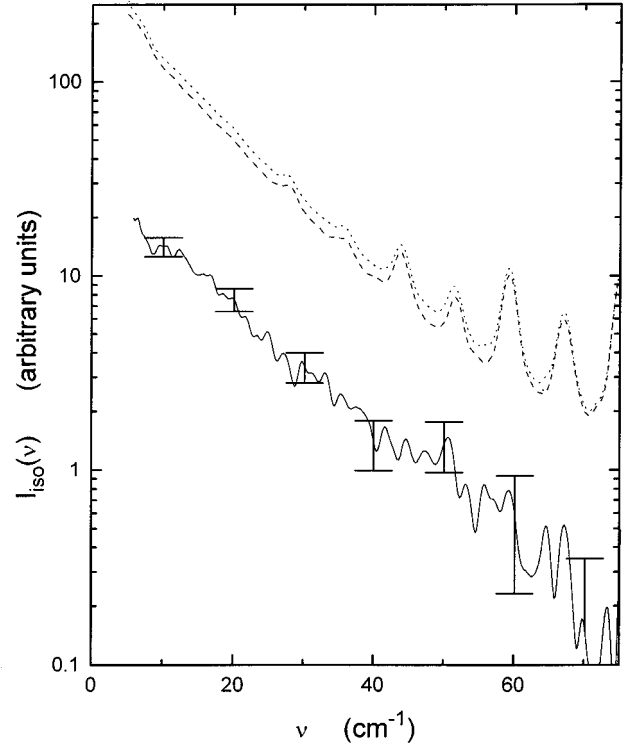


FIG. 1. Experimental spectra:  $I_{VV}$  (dotted line),  $\frac{4}{3}I_{HV}$  (dashed line),  $I_{\text{iso}}$  (solid line). In  $I_{\text{iso}}$  the estimated error bars are reported.

Figure 1 shows the Stokes side of the  $I_{VV}(\nu)$  and  $I_{HV}(\nu)$  measured spectra, together with the evaluated  $I_{\text{iso}}(\nu)$  experimental spectrum, in logarithmic scale for  $\rho_{\text{Hg}} = 0.113$  atom/nm<sup>3</sup> and  $\rho_{N_2} \approx \rho_{\text{Hg}}/3$  molecules/nm<sup>3</sup>. For clarity  $I_{HV}$  has been multiplied by  $\frac{4}{3}$ . It is evident that at high frequency, where the nitrogen contribution is dominant in both spectra,  $I_{VV}$  and  $\frac{4}{3}I_{HV}$  superimpose each other within the experimental uncertainties and the  $I_{\text{iso}}$  spectrum is practically vanishing at frequencies higher than 70 cm<sup>-1</sup>. For frequencies below 70 cm<sup>-1</sup> the clear difference between  $I_{VV}$  and  $\frac{4}{3}I_{HV}$  manifests the presence of a collision-induced isotropic contribution. The rotational lines disappear in the obtained  $I_{\text{iso}}$  spectrum between 6 and 70 cm<sup>-1</sup> within the error bars.

The precise absolute calibration of pair spectrum  $I_{\text{iso}}$  has been determined by comparison with the depolarized spectrum [11] and controlled with the intensity of the high-frequency rotational lines of nitrogen.

The values of the experimental zeroth and second moments of  $I_{\text{iso}}$  have been calculated by means of the standard expressions:

$$M_n^{\text{iso}} = \int_{-\infty}^{+\infty} \nu^n I_{\text{iso}}(\nu) d\nu \quad (2)$$

and are given in Table I.  $I_{\text{iso}}(\nu)$  is related to the double differential scattering cross section for the diatom and is given by the theoretical expression [7]

$$I_{\text{iso}}(\nu) = V \frac{d^2 \sigma_{\text{iso}}}{d\Omega d\nu} = V k_0 k_s^3 \int_{-\infty}^{+\infty} dt \exp(-i2\pi\nu t) \times \langle a[r(t)]a[r(0)] \rangle, \quad (3)$$

TABLE I. Calculated and experimental moments of the collision-induced isotropic light-scattering spectrum of a mercury diatom at  $T=973$  K. The calculations are performed with the *MSKAK* pair potential [16].

	$M_0^{\text{iso}}$ ( $10^{-49}$ cm $^5$ )	$M_2^{\text{iso}}$ ( $10^{-49}$ cm $^3$ )	$M_2^{\text{iso}}/M_0^{\text{iso}}$ (cm $^{-2}$ )
DID—first	0.237	165	697
DID—all	0.322	291	904
Empirical	0.199	91	457
Experimental	$0.20 \pm 0.03$	$94 \pm 10$	$458 \pm 10$

where  $V$  stands for the volume of the scattering system,  $a(r(t))$  for the trace of I-I polarizability of the pair at distance  $r$  and time  $t$ , and the angular brackets stand for equilibrium ensemble average. The frequency and wave vector of the incoming and scattered light are  $\nu_0, k_0$ , and  $\nu_s, k_s$ , respectively;  $\nu = \nu_0 - \nu_s$  stands for the frequency shift.

Once a model form for the pair potential and pair polarizability trace are given, theoretical calculations of zeroth and second moments, within the framework of classical mechanics which is appropriate for dealing with heavy atoms, such as mercury, at high temperature, can easily be performed by

$$M_0^{\text{iso}} = \int_{-\infty}^{+\infty} I_{\text{iso}}(\nu) d\nu \approx k_0^4 \int_V g(r) a^2(r) 4\pi r^2 dr, \quad (4)$$

$$M_2^{\text{iso}} = \int_{-\infty}^{+\infty} \nu^2 I_{\text{iso}}(\nu) d\nu \approx \frac{2k_B T}{m} k_0^4 \int_V g(r) \left( \frac{da(r)}{dr} \right)^2 4\pi r^2 dr, \quad (5)$$

where  $m$  is the atomic mass,  $g(r)$  is the pair distribution function, and we have approximated  $k_s \sim k_0$ .

For the sake of comparison and discussion, we have first calculated the zeroth and second moments of  $I_{\text{iso}}(\nu)$  by using Eqs. (4) and (5) and two elementary models of the pair polarizability trace, i.e., the lowest-order and all-order DID approximations [14] plus the hyperpolarizability term [15] given by

$$a(r) = (4\alpha^3 + 5\gamma C_6/9\alpha)/r^6, \quad (6)$$

$$a(r) = \frac{4\alpha^3}{r^6 - \alpha r^3 - 2\alpha^2} + \frac{5\gamma C_6}{9\alpha r^6}, \quad (7)$$

where  $\alpha$  stands for the particle polarizability,  $\gamma$  for the second hyperpolarizability, and  $C_6$  for the first dispersion force coefficient. The use of the all-order DID term for the trace could be justified here by the fact that the ratio  $(\alpha/r_m^3)$  is large for mercury and determines the importance of the successive terms in the dipolar series expansion.

Table I gives the comparison between the experimental moments of  $I_{\text{iso}}(\nu)$  derived from the measured spectrum following Eq. (2) and the moments calculated by using the two expressions for the polarizability trace, Eqs. (6) and (7) and Eqs. (4) and (5), with  $\gamma \approx 8 \times 10^{12}$  Å $^6$  erg $^{-1}$  ( $1 \times 10^{-60}$

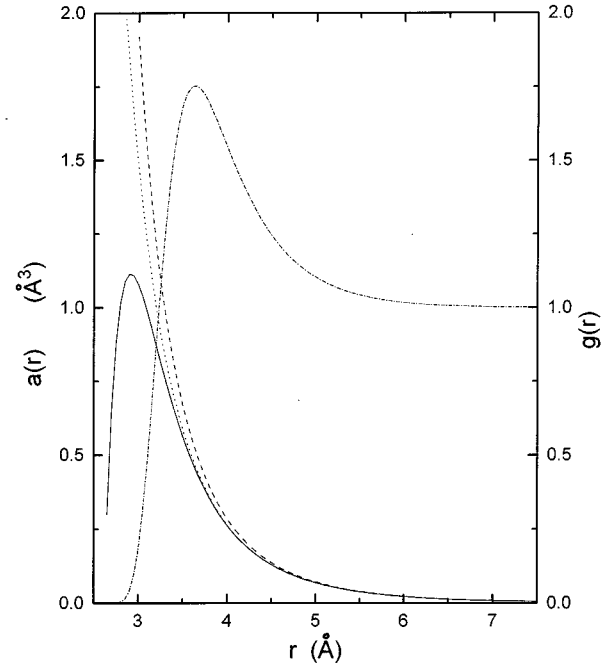


FIG. 2. The induced polarizability trace of a mercury diatom as a function of pair distance: lowest-order DID (dotted line), all-order DID (dashed line), empirical model (full line). The pair distribution function  $g(r)$  in the low-density limit at  $T=973$  K for the *MSKAK* pair potential has also been reported (dashed-dotted line).

C $^4$  m $^4$  J $^{-3}$ ) and  $C_6 \approx 4 \times 10^{-10}$  Å $^6$  erg ( $4 \times 10^{-77}$  m $^6$  J) [12] and the *MSKAK* pair potential [16].

The inadequacy of both models of the trace for the correct description of the experimental results is clear from the comparison, mainly because these models do not reproduce the normalized second moment  $M_{2,n} = M_2/M_0$  (as well as  $M_2$ ).  $M_{2,n}$  is related to the square of the decay constant of the almost exponential  $I_{\text{iso}}(\nu)$  spectrum and can be determined experimentally with good precision, not being affected by calibration errors. Both models give  $M_{2,n}$  values much higher than the experimental ones and well outside the experimental uncertainties. The experimental value of  $M_0$  being about 20% smaller than the lowest-order DID one indicates that a negative short-range term must be added to  $a(r)$  to reconcile the calculations with the experiment. This is similar to what happens to the induced anisotropy of noble gases [17].

In agreement with previous works [7] we have adopted the following empirical model of the trace of a mercury diatom:

$$a(r) = (4\alpha^3 + 5\gamma C_6/9\alpha)/r^6 - B \exp(-r/r_0) \quad (8)$$

and determined the parameters  $B$  and  $r_0$  by fitting the calculated  $M_0$  and  $M_2$  to the experimental values. The best fit gives  $B \approx 7 \times 10^6$  Å $^3$  and  $r_0 \approx 0.18$  Å. The moments corresponding to the empirical polarizability trace are also reported in Table I. Figure 2 shows the behavior of the three different induced polarizability traces  $a(r)$  together with the pair correlation function in the low-density limit,  $g(r) = \exp[-U(r)/k_B T]$ , for the *MSKAK* pair potential  $U(r)$  at  $T=973$  K. The range of  $r$  where  $g(r)$  is significantly

different from zero defines the region probed by our experiment. We remark that the difference between the empirical and lowest-order DID models is significant only below 4 Å, a range much shorter than the corresponding one in modeling the anisotropic part of I-I polarizability [12]. In addition, similarly to what happens for the polarizability anisotropy, the trace also behaves quite differently from the traces of noble gases which all become negative at a distance  $r \sim r_m$  [18]. In the case of mercury the trace is large and positive

down to  $\sim 0.8r_m$ , indicating the existence of a contribution due to strong electron correlation effects in the overlap region, which is known to be positive for both trace and anisotropy [18], thus confirming what has already been found for the I-I polarizability anisotropy of a mercury diatom.

We are gratefully indebted to Dr. Jorg Rathenow and Lorenzo Grassi for technical collaboration during the experiment.

- 
- [1] *Phenomena Induced by Intermolecular Interactions*, edited by G. Birnbaum (Plenum, New York, 1985).
- [2] For a recent review see *Collision- and Interaction-Induced Spectroscopy*, edited by G. C. Tabisz and M. N. Neuman (Kluwer, Dordrecht, 1995).
- [3] M. H. Proffitt, J. W. Keto, and L. Frommhold, *Phys. Rev. Lett.* **45**, 1843 (1980).
- [4] A. De Santis and M. Sampoli, *Chem. Phys. Lett.* **96**, 114 (1983).
- [5] P. D. Dacre and L. Frommhold, *J. Chem. Phys.* **76**, 3447 (1982).
- [6] In previous works on noble gases [3,5], the spectrum due to the I-I polarizability trace has been called the “polarized spectrum.” Here “polarized spectrum” stands for the scattered intensity with polarization equal to that of the incoming beam.
- [7] L. Frommhold, *Adv. Chem. Phys.* **46**, 1 (1981).
- [8] M. Sampoli, A. Guasti, F. Barocchi, R. Winter, J. Rathenow, and F. Hensel, *Phys. Rev. A* **42**, 6910 (1992).
- [9] F. Barocchi, M. Sampoli, F. Hensel, J. Rathenow, and R. Winter, in *Proceedings of the Eighth International Conference on Liquid and Amorphous Metals*, edited by J. Hafner [J. Non-Cryst. Solids **156-158**, 663 (1993)].
- [10] F. Barocchi, M. Sampoli, F. Hensel, J. Rathenow, and R. Winter, in *Proceedings of the NATO Advanced Research Workshop on Collision- and Interaction-Induced Spectroscopy*, edited by G. C. Tabisz and M. N. Neuman (Kluwer, Dordrecht, 1995).
- [11] M. Sampoli, F. Barocchi, L. Grassi, F. Hensel, and J. Rathenow, *Europhys. Lett.* **28**, 483 (1994).
- [12] F. Barocchi, F. Hensel, and M. Sampoli, *Chem. Phys. Lett.* **232**, 445 (1995).
- [13] C. M. Penny, S. T. Peters, and M. Lapp, *J. Opt. Soc. Am.* **64**, 712 (1974); N. J. Bridge and A. D. Buckingham, *Proc. R. Soc. London, Ser. A* **295**, 334 (1968).
- [14] L. Silberstein, *Philos. Mag.* **33**, 521 (1917).
- [15] A. D. Buckingham, *Trans. Faraday Soc.* **52**, 1035 (1956).
- [16] J. Koperski, J. B. Atkinson, and L. Krause, *Chem. Phys. Lett.* **219**, 161 (1994).
- [17] N. Meinander, G. C. Tabisz, and M. Zoppi, *J. Chem. Phys.* **84**, 3005 (1986).
- [18] P. D. Dacre, *Mol. Phys.* **45**, 1 (1982); **45**, 17 (1982); **47**, 193 (1982).